Large eddy simulation of shock turbulence interaction

By S. Lee

1. Motivations and objectives

The presence of shock waves is an important feature that distinguishes high-speed flows from low-speed ones. Understanding the mechanisms of turbulence interacting with a shock wave is not only of generic interest, but also of fundamental importance in predicting the interactions of turbulent boundary layers with shock waves which occur in many practical engineering applications. Many flows of interest have very high Reynolds numbers with large ranges of dynamic scales which cannot be captured by direct numerical simulation (DNS). Large eddy simulation (LES) is thus required where the large scale structures are resolved and the effects of the small, unresolved "subgrid" scales on the larger, resolved scales are modeled. The cost of resolving the shock wave structure is extremely prohibitive for a strong shock wave (Lee *et al.* 1992). Therefore, a numerical method is required which can predict changes of flow variables across the shock wave without resolving the structure. The method is required to have high order numerical accuracy in smooth regions of the flow domain to properly predict the evolution of turbulence.

A new subgrid-scale (SGS) model was developed by Germano *et al.* (1991) that augments the standard Smagorinsky (1963) eddy viscosity model by replacing the *ad hoc*, flow dependent constant with a coefficient determined by the resolved scales in the LES. The coefficient automatically adjusts to the flow conditions. This "dynamic" SGS model has been extended by Moin *et al.* (1991) to the simulation of compressible turbulence and passive scalar transport. Recently, Ghosal *et al.* (1992) developed SGS models which eliminate some inconsistencies in the previous dynamic models.

A shock capturing scheme developed by Harten *et al.* (1987) is essentially non-oscillatory (ENO), which can also be constructed to be high order accurate throughout the domain. The non-oscillatory nature of the scheme is achieved by choosing a interpolating stencil which gives the smoothest evaluation of the derivatives of the primitive variables. Shu and Osher (1989) extended the scheme to interpolate the fluxes instead of the primitive variables, which significantly simplifies the scheme.

The immediate goal of this work is two-folds: to test the performance of LES calculation performed with a conservative formulation, a formulation preferred in the shock-involved simulations, and to test the performance of the shock capturing scheme and validate the scheme against the DNS by Lee *et al.* (1992) for a weak shock wave.

An immediate extension of the present work is to perform DNS of low Reynolds number turbulence interacting with strong shock waves by using the shock capturing scheme. Understanding the interaction of high Reynolds number turbulence with shock waves through LES is the long range goal of this work.

2. Accomplishments

A nonconservative formulation of the energy equation (solving for internal energy) was used to perform large eddy simulations of compressible turbulence in Moin *et al.* (1991) due to its simplicity in implementing SGS models compared to the conservative formulation (solving for total energy). In problems with shocks in the domain, however, the total energy formulation is preferred due to its conservative nature. A conservative set of equations for the LES were derived from the nonconservative equations derived by Moin *et al.* (1991). Performance of the conservative formulation was compared with the experiment on decaying grid-generated turbulence as well as with the filtered DNS field, which is reported in §2.1. Various shock-capturing schemes were tested, and an ENO shock-capturing scheme of Shu and Osher (1989) was chosen for the simulation of shock/turbulence interaction. The scheme was tested and validated against the data base generated by DNS of weak shock waves, which is reported in §2.2. The results obtained with the ENO scheme were within 5% from the DNS results, and used less than 25% of the CPU time used in the DNS.

2.1 LES with a conservative formulation

In the LES of compressible simulation by Moin *et al.* (1991), nonconservative energy equation was used due to its simple form. The equations used are

$$\frac{\partial \overline{\rho}}{\partial t} + \frac{\partial \overline{\rho}\widetilde{u}_k}{\partial x_k} = 0,$$

$$\frac{\partial \overline{\rho}\widetilde{u}_i}{\partial t} + \frac{\partial \overline{\rho}\widetilde{u}_i\widetilde{u}_k}{\partial x_k} = -\frac{\partial \overline{p}}{\partial x_i} + \frac{\partial \sigma_{ik}}{\partial x_k} - \frac{\partial \tau_{ik}}{\partial x_k},$$

$$\frac{\partial \overline{\rho} c_v \widetilde{T}}{\partial t} + \frac{\partial \overline{\rho} c_v \widetilde{T}\widetilde{u}_k}{\partial x_k} = -\overline{p}\frac{\partial \widetilde{u}_k}{\partial x_k} + \sigma_{ik}\frac{\partial \widetilde{u}_k}{\partial x_i} - c_v\frac{\partial q_k}{\partial x_k},$$

where σ_{ik}, τ_{ik}, and q_k represent the resolved viscous stress, the subgrid-scale stress, and heat flux,

$$\sigma_{ik} = \overline{\mu}\left(\frac{\partial \widetilde{u}_i}{\partial x_k} + \frac{\partial \widetilde{u}_k}{\partial x_i} - \frac{2}{3}\frac{\partial \widetilde{u}_m}{\partial x_m}\delta_{ik}\right)$$

$$\tau_{ik} = \overline{\rho}(\widetilde{u_i u_k} - \widetilde{u}_i\widetilde{u}_k)$$

$$q_k = \overline{\rho}(\widetilde{u_k T} - \widetilde{u}_k\widetilde{T}),$$

respectively. The overbar denotes the filtering operation, and the tilde denotes the density-weighted filter. The filtering operations always refer to a sharp cutoff (or volume-weighted average) in the homogeneous direction of the flow. The subgrid scale stress τ_{ik} and heat flux q_k were determined through the dynamic procedure suggested by Germano *et al.* (1991). Derivation of the energy equation for the LES using the conservative formulation introduces terms which are complex to model, for example, the subgrid scale convection of the total energy (sum of thermal and kinetic energy) needs to be modeled.

However, if the resolved total energy ($\overline{E}_T$) is defined as

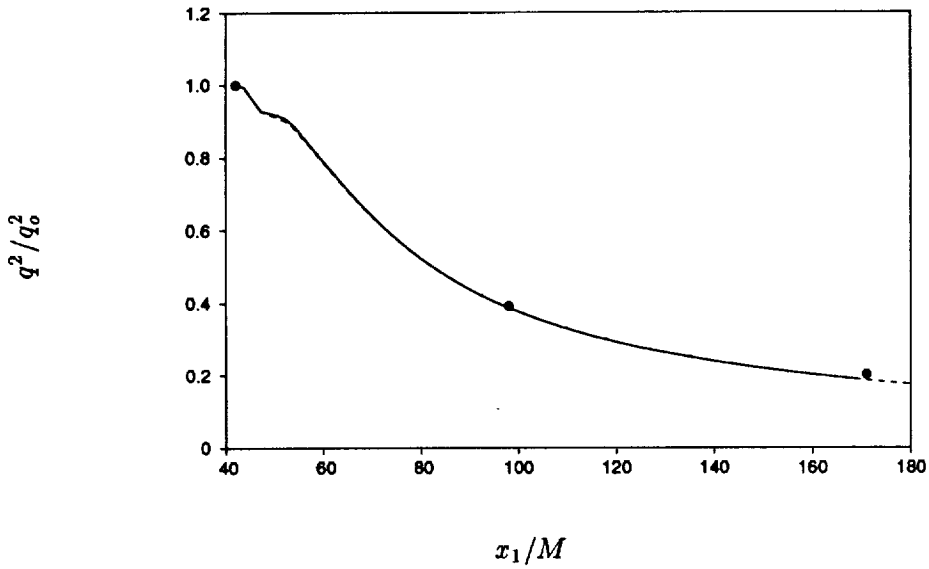

FIGURE 1. Evolution of resolved turbulent kinetic energy. • filtered experiment (Comte-Bellot & Corrsin 1971), —— LES with conservative formulation, ---- LES with nonconservative formulation.

$$\overline{E}_T = \overline{\rho}(c_v\widetilde{T} + \widetilde{u}_k\widetilde{u}_k/2)$$

rather than $\overline{\rho}(c_v\widetilde{T} + \widetilde{u_k u_k}/2)$, the conservative energy equation can be derived from the nonconservative equations presented above, and the extra complexities can be circumvented. The resulting energy equation becomes

$$\frac{\partial\overline{E}_T}{\partial t} + \frac{\partial\overline{E}_T\widetilde{u}_k}{\partial x_k} = -\frac{\partial\overline{p}\widetilde{u}_k}{\partial x_k} + \frac{\partial\sigma_{ik}\widetilde{u}_k}{\partial x_i} - \widetilde{u}_k\frac{\partial\tau_{ik}}{\partial x_i} - c_v\frac{\partial q_k}{\partial x_k},$$

The terms to be modeled remain the same and are parametrized as

$$\tau^*_{ik} = \overline{\rho}C_S\Delta^2|\widetilde{S}|\widetilde{S}^*_{ik},$$
$$q^2 = \overline{\rho}C_I\Delta^2|\widetilde{S}|^2,$$
$$q_k = \overline{\rho}D\Delta^2|\widetilde{S}|\widetilde{T}_{,k},$$

where $q^2 = \tau_{mm}$ and $\tau^*_{ik} = \tau_{ik} - q^2\delta_{ik}/3$. The detailed procedures of dynamically determining coefficients, C_S, C_I, and D, are described in Moin *et al.* (1991). The concept of least squares suggested by Lilly (1992) replaced the rather arbitrary procedure of determining scalar coefficients, C_S and D, from the tensor or vector relations.

The experiment on the decay of grid-generated turbulence with $Re_\lambda = 71.6$ (Comte-Bellot and Corrsin 1971) was simulated as a temporal decay with $32\times32\times32$

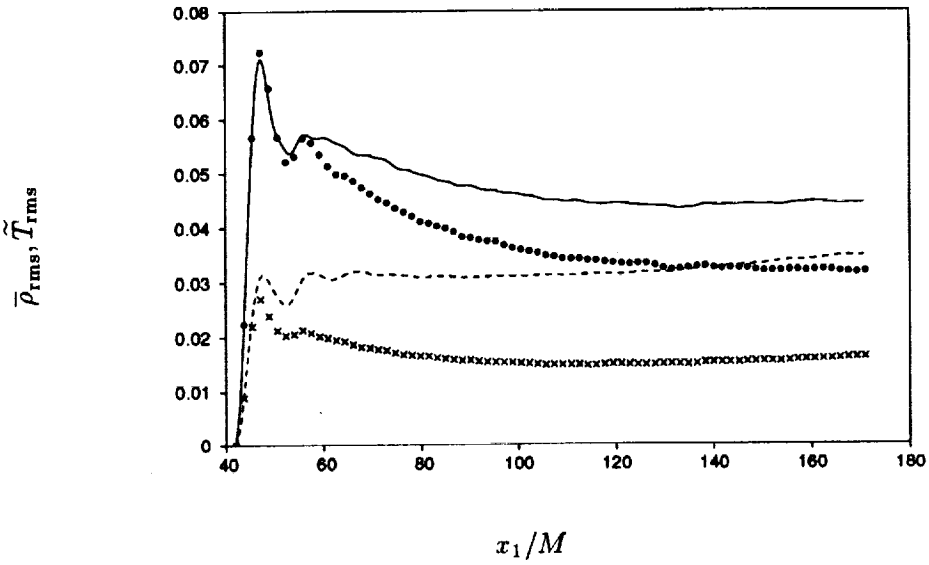

FIGURE 2. Evolution of resolved density and temperature fluctuations. Conservative formulation: ——— density, ---- temperature, nonconservative formulation: • density, × temperature.

grid points with different formulations. Decay of the resolved scale TKE is compared in Figure 1. The evolution is insensitive to the choice of the formulation. Evolutions of *rms* density and temperature fluctuations are compared in Figure 2. (The fluctuations in thermodynamic quantities were initially set to zero.) Even though the evolution of velocity field does not depend significantly on the choice of the formulation, the evolution of density fluctuation depends on this choice.

To check if this dependence is due to the initial transient of the fluctuation density field, LES's of decaying compressible turbulence ($Re_\lambda = 35, M_t = 0.61$, where eddy-shocklets were found in DNS) were performed. Initial conditions of the simulation were taken as the Fourier filtered DNS field onto $32 \times 32 \times 32$ grids at $t/\tau_t \simeq 0.85$, when turbulence is fully developed in every respect. Figure 3 shows evolution of *rms* density fluctuation from the two formulations, which shows good agreement between the two and with the filtered DNS.

The reason for the different evolution of density field shown in Figure 2 is not yet fully understood. Some possible reasons are: (1) aliased evaluation of temperature in the conservative formulation ($\overline{\rho}\widetilde{u}_k\widetilde{u}_k$ is subtracted from $\overline{E}_T$), (2) different initial transient to set up temperature fluctuations. Before conducting the LES of shock/turbulence interaction, validity of the formulation and the SGS models should be established.

2.2 Development of an ENO scheme

For a strong shock wave, resolving the shock structure by solving Navier-Stokes equations is irrelevant because Navier-Stokes equations are no longer valid inside

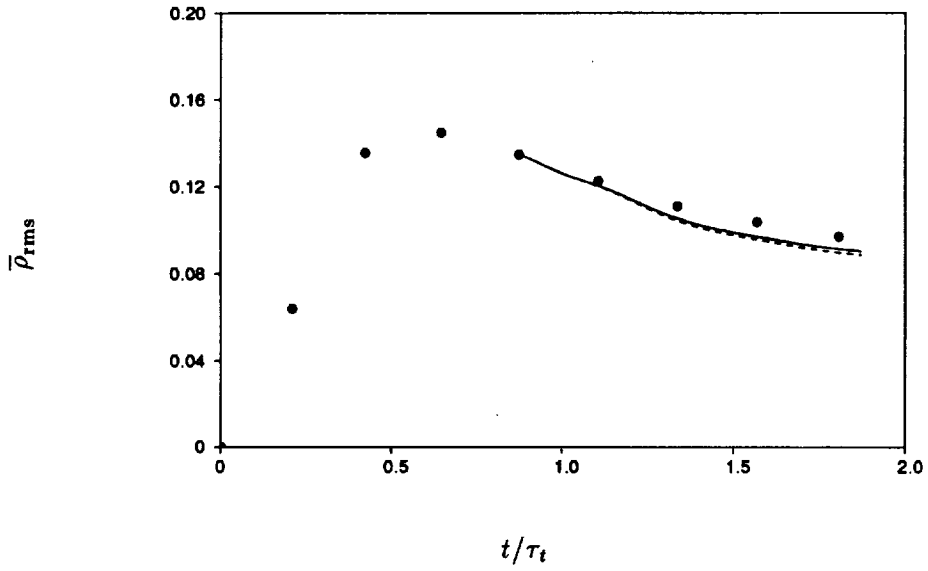

FIGURE 3. Evolution of resolved density fluctuation. • filtered DNS (Lee *et al.* 1992), —— LES with conservative formulation, ---- LES with nonconservative formulation.

the shock wave with $M_1 > 2.0$. (Sherman 1955) Therefore, there is no point to resolving the structure of the strong shock wave with the expense of huge computational cost. A shock-capturing scheme is implemented for the simulation of strong shock wave/turbulence interaction. In simulations of shock/turbulence interaction, a shock capturing scheme is required to be high order accurate throughout the computational domain (to properly simulate the turbulence evolution) as well as to be able to give smooth and accurate transition across the shock wave. The shock-capturing scheme of the choice is the essentially non-oscillatory (ENO) scheme, which can be constructed up to any order of accuracy. The ENO scheme used in this work is based on the Lax-Friedrichs scheme with interpolation of fluxes (Shu and Osher, 1989). Some modifications are made to the basic scheme to improve the solution accuracy and to enhance the code performance.

For the sake of completeness, the *basic* ENO scheme is briefly described in the following. The three-dimensional, compressible Navier-Stokes equation can be written as

$$\mathbf{q}_t + \mathbf{f}(\mathbf{q})_x + \mathbf{g}(\mathbf{q})_y + \mathbf{h}(\mathbf{q})_z = \mathbf{V},$$

where,

$$\mathbf{q} = (\rho, \rho u_1, \rho u_2, \rho u_3, E_T)^T,$$
$$\mathbf{f}(\mathbf{q}) = u_1\mathbf{q} + p(0, 1, 0, 0, u_1)^T,$$
$$\mathbf{g}(\mathbf{q}) = u_2\mathbf{q} + p(0, 0, 1, 0, u_2)^T,$$
$$\mathbf{h}(\mathbf{q}) = u_3\mathbf{q} + p(0, 0, 0, 1, u_3)^T,$$

and $\mathbf{V}$ is the molecular diffusion terms.

The ENO adaptive-stencil procedure is applied only to the convection terms (the left-hand side of the above equation). The diffusion terms are approximated by the sixth-order Pade scheme, which is the base scheme used in the shock-resolving direct numerical simulation (Lee *et al.* 1992). The time advancement is performed by a third order Runge-Kutta method. Three convection terms are approximated dimension-by-dimension: for example, when approximating $\mathbf{f}(\mathbf{q})_x$, y and z are fixed. The core algorithm is then a one-dimensional ENO approximation to $\mathbf{f}(\mathbf{q})_x$.

The flux vector $\mathbf{f}(\mathbf{q})_x$ can be approximated either by component by component or in characteristic directions, but for simplicity of implementation, the component treatment was chosen. To obtain nonlinear stability by upwinding, $\mathbf{f}(\mathbf{q})_x$ is decomposed into

$$\mathbf{f}(\mathbf{q})_x = \mathbf{f}^+(\mathbf{q})_x + \mathbf{f}^-(\mathbf{q})_x$$

with

$$\mathbf{f}^\pm(\mathbf{q})_x = (\mathbf{f}(\mathbf{q})_x \pm \alpha\mathbf{q})/2,$$

where $\alpha = \max(|u_1| + c)$ (c is the sound speed) is the largest eigenvalue in absolute value of the Jacobian $\partial\mathbf{f}/\partial\mathbf{q}$ along the relevant x-line. The decomposition guarantees that $\partial\mathbf{f}^\pm/\partial\mathbf{q}$ has positive/negative eigenvalues. Therefore, upwinding (to be discussed) is the same for all components of the flux.

Suppose f is a component of the flux $\mathbf{f}^\pm(\mathbf{q})$. $f(\mathbf{q})_x$ is written as a conserved flux difference

$$f_x\big|_{x=x_j} \simeq \frac{1}{\Delta x}(\hat{f}_{j+\frac{1}{2}} - \hat{f}_{j-\frac{1}{2}}),$$

where the numerical flux $\hat{f}_{j+1/2}$ approximates $h(x_{j+1/2})$ to a high order with $h(x)$ defined by

$$f(u(x)) = \frac{1}{\Delta x}\int_{x-\frac{\Delta x}{2}}^{x+\frac{\Delta x}{2}} h(\xi)d\xi.$$

In order to evaluate the numerical flux $\hat{f}_{j+1/2}$, $h(x)$ need not to be explicitly constructed. The numerical fluxes can be expressed in terms of the undivided differences of $f(u(x))$ as

$$\hat{f}_{j+1/2} = \sum_{m=0}^{r} c(i-j, m)f[i, m],$$

with i being the left-most point in the stencil used to approximate $\hat{f}_{j+1/2}$, and $c(s,m)$ and the undivided difference $f[j,k]$ being defined by

$$c(s,m) = \frac{1}{(m+1)!} \sum_{l=s}^{s+m} \prod_{\substack{p=s \\ p \neq l}}^{s+m} (-p)$$

and

$$f[j,0] = f(u_j),$$
$$f[j,k] = f[j+1,k-1] - f[j,k-1], \qquad k = 1,...,r$$

respectively.

The adaptive stencil (represented by i) is determined by the following procedure.
(1) Start with $i = j$ or $i = j+1$ according to the local upwinding direction.
(2) For k-th level of approximation,

$$i = i - 1 \text{ if } |f[i,k]| > |f[i-1,k]| \qquad \text{for } k = 1,...,r.$$

The ENO scheme was implemented in the code developed for the simulation of shock/turbulence interaction. Simulation of spatially decaying turbulence was performed (1) to validate the scheme and (2) to determine the required order of the ENO scheme to reproduce the quality of the corresponding DNS. In the validation procedure, a totally unexpected accuracy degeneracy was noticed with the increase of the ENO scheme's order. As the order of the ENO increases, the solution deviates further from the DNS solution. Similar accuracy degeneracy was reported by Rogerson and Meiburg (1990) while they were refining the grid. This degeneracy was due to the choice of linearly unstable stencils during the adaptive ENO procedure (Shu 1990). This phenomenon is more pronounced for the higher order scheme with more refined grid. A biasing toward the central difference stencil (Shu 1990) was implemented to avoid the accuracy degeneracy in smooth regions. With this fix, by raising the order of accuracy, more accurate results could be obtained. Results comparable to the corresponding DNS (with sixth-order Pade scheme) was obtained when the accuracy of the ENO scheme was sixth order. Beyond the sixth-order, the effect of the increased order was found negligible in this case.

The operation count and, accordingly, the CPU time are increased a few times compared to the standard DNS code when the ENO scheme is implemented throughout the domain. The region where the ENO scheme plays a significant role is quite localized, usually less than a tenth of the computational domain in DNS of weak shock waves, and is expected to be even smaller for stronger shock waves. The idea of applying the ENO scheme only where it plays an active role and switching elsewhere into the usual Pade central difference was tested in pursuit of saving unnecessary computer usage. The local region of ENO application can even be specified *a priori* to be a zone around the shock since the simulation is performed in a coordinate system fixed on the mean shock wave. The concept of local application of the ENO scheme was validated against fully resolved DNS results both for the case of two-dimensional shock/turbulence interaction with $M_1 = 1.2$, $M_t = 0.07$ and the case of three-dimensional spatially decaying turbulence with $M_t = 0.51$ and

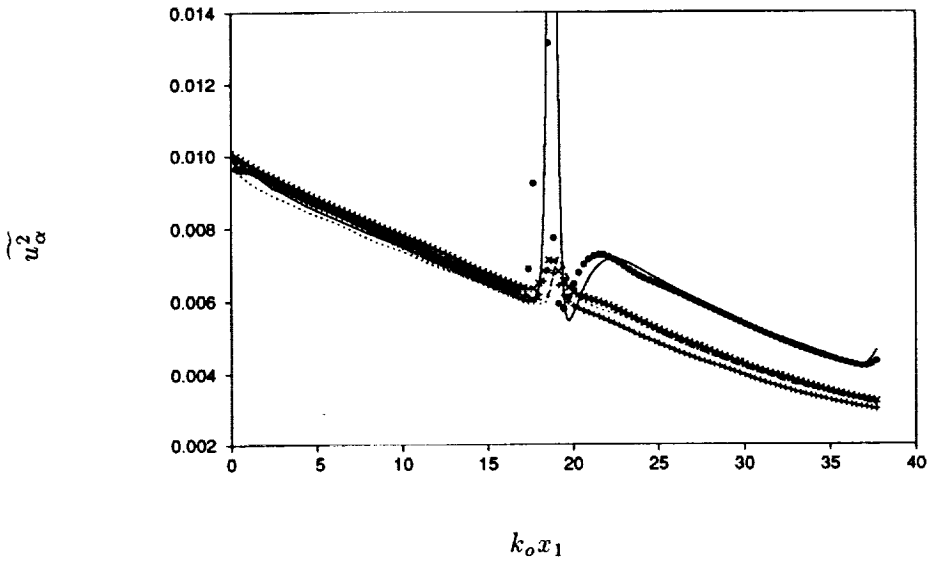

FIGURE 4. Evolution of velocity fluctuations in three-dimensional shock/turbulence interaction. Lines denote DNS results and symbols denote results using the ENO scheme. u_1 (——— , •), u_2 (---- , ×), u_3 (····· , +).

$Re_\lambda = 25$. For the two-dimensional shock/turbulence case with $M_1 = 1.2$, CPU time required was reduced to a third of the corresponding DNS and is expected to be larger for the stronger shock waves.

The next validation was to simulate the three-dimensional shock/turbulence interaction using the ENO scheme near the shock and the Pade scheme elsewhere. Significant additional decay of TKE was found in the shock vicinity where the ENO scheme is applied, which was not pronounced in two-dimensional shock/turbulence simulations. The excessive TKE dissipation in the ENO zone was suspected to be from the additional dimension (x_3-direction) for the ENO procedure. In order to investigate the effect of the dimensions, the ENO scheme was applied only in the shock-normal direction for the two-dimensional shock/turbulence simulation. More accurate results were obtained with less CPU time used. For $M_1 = 1.2$, the ENO scheme required only a quarter of the CPU time used in the corresponding DNS.

The final ENO scheme developed in this work interpolates (up to sixth-order) fluxes based on Lax-Friedrichs method with biasing the interpolation stencil toward the central differencing. The ENO procedure is applied only to the convection terms in the shock-normal direction. The ENO scheme is made only active near the shock wave and switched into the sixth-order Pade scheme elsewhere.

The final validations were made for two cases: (1) three-dimensional turbulence interacting with a weak shock wave ($M_1 = 1.2$) and (2) two-dimensional turbulence interacting with a relatively strong shock wave ($M_1 = 2.0$). The first case was chosen to check the performance of the ENO scheme in three-dimensional case, and

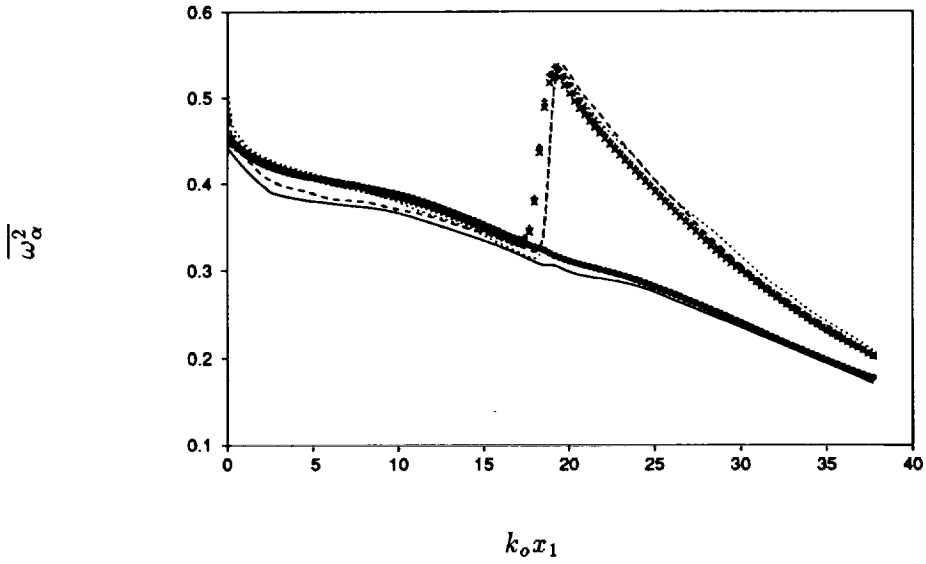

FIGURE 5. Evolution of vorticity fluctuations in three-dimensional shock/turbulence interaction. Lines denote DNS results and symbols denote results using the ENO scheme. ω_1 (——— , •), ω_2 (---- , ×), ω_3 (····· , +).

the result was compared with the corresponding DNS result (Lee *et al.* 1992). The second case was chosen to check the accuracy of the ENO scheme for strong shock waves. For the purpose of comparison, a shock-resolving DNS of two-dimensional shock/turbulence interaction was also performed.

As a validation of the ENO scheme for three-dimensional shock/turbulence interaction, reproduction of the DNS results of Case C in Lee *et al.* (1992) was tried where $M_1 = 1.2$, $M_t = 0.095$, and $Re_\lambda = 12$ just upstream of the shock. In the DNS, $193 \times 64 \times 64$ grids (with significant grid refinement near the shock) and 160 Cray/Y-MP CPU hours were used to give marginally converged statistics. In the ENO scheme, $129 \times 64 \times 64$ uniform grids and 40 Cray/Y-MP CPU hours were used for the same quality of statistics.

Figure 4 compares the evolution of velocity fluctuations obtained by DNS and ENO in three-dimensional shock/turbulence interaction. Except for the position of the mean shock wave, the amplification and free evolution of velocity from DNS are well reproduced by the ENO scheme. Since the ENO scheme is activated in the shocked zone, the peak *rms* fluctuations inside the shock wave due to the shock intermittency are not expected to agree with the DNS.

Figure 5 compares vorticity component evolution obtained by DNS and ENO. Once the shift of the mean shock position is considered, predictions by the ENO scheme are in excellent agreement with the DNS results. Other turbulence quantities, such as fluctuations in dilatation, density, and temperature, were in good agreement with the DNS results outside the zone occupied by the shock wave.

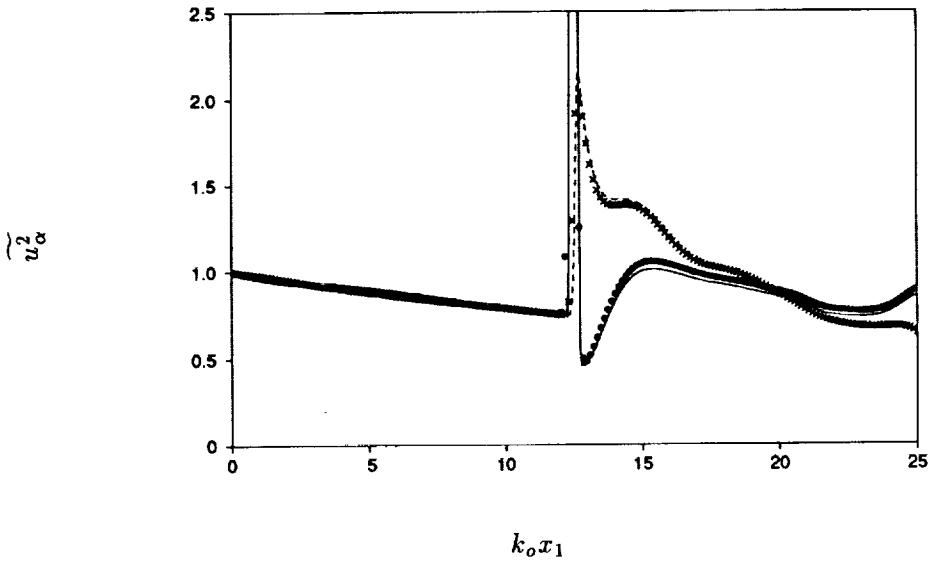

FIGURE 6(A). Evolution of velocity fluctuations in two-dimensional shock/turbulence interaction. Lines denote DNS results and symbols denote results using the ENO scheme. u_1 (——— , •), u_2 (---- , ×).

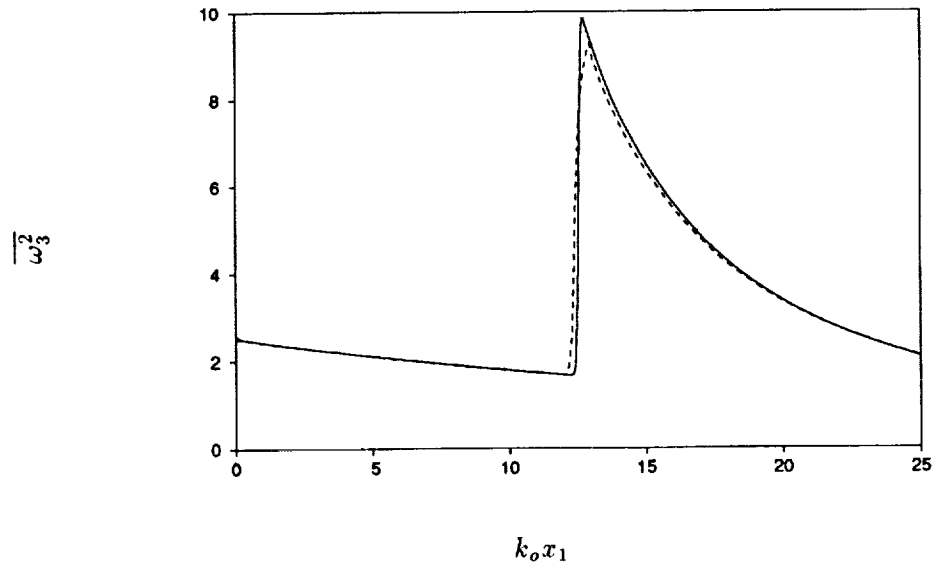

FIGURE 6(B). Evolution of vorticity fluctuations in two-dimensional shock/turbulence interaction. ——— DNS, ---- ENO.

As a validation of the ENO scheme for shock/turbulence interaction at high Mach numbers, results of the ENO scheme on two-dimensional shock/turbulence interaction was compared with the corresponding DNS, where $M_1 = 2.0$ and $M_t = 0.07$ at the inflow. The minimum grid spacing required by the ENO scheme was five times larger than that used in the DNS. Figure 6(a) and (b) compare velocity and vorticity fluctuations from the ENO scheme with those from the DNS. The jumps and evolutions behind the shock wave were reproduced by the ENO scheme with much less cost than the DNS. The results from the ENO scheme are indeed dependent on the resolution near the shock wave, and a grid-refinement test was performed before comparing the results. In order to accurately predict the interaction of turbulence with the stronger shock waves, where no DNS results are available, a grid in the shock vicinity should be refined until the result is no longer dependent on further grid refinement.

3. Future plans

Further tests of the LES with the conservative formulation against the filtered DNS and LES with the nonconservative formulation will continue. Extension of Ghosal *et al.*'s (1992) model (a constrained integral equation approach and a SGS model using transport equation for SGS turbulent kinetic energy) to compressible turbulence will also be performed.

In most DNS and LES of compressible turbulence, aliasing errors were controlled rather than clearly removed. In Lee *et al.* (1992), it was proposed to solve a continuity equation in terms of specific volume instead of density to completely remove aliasing errors. A simulation with this formulation will be executed. The simulation can be used as a reference to investigate the accuracy of the existing formulations.

Interaction of three-dimensional isotropic turbulence with strong shock waves will be performed to study the effect of the shock strength. Once SGS models and formulations are developed and validated, LES of turbulence interacting with shock waves of various strengths will also be performed.

REFERENCES

COMTE-BELLOT, G. & CORRSIN, S. 1971 Simple Eulerian time correlation of full and narrow band velocity signals in grid generated, isotropic turbulence. *J. Fluid Mech.* **48,** 273-337.

GERMANO, M., PIOMELLI, U., MOIN, P., & CABOT, W. 1991 A dynamic subgrid-scale eddy-viscosity model. *Phys. Fluids A.* **3,** 1760-1765.

GHOSAL, S., LUND, T. S., & MOIN, P. 1992 A dynamic localization model for large-eddy simulation of turbulent flows. *CTR Ann. Res. Brief-1992*, Stanford Univ./NASA Ames.

HARTEN, A., ENQUIST, B., OSHER, S., & CHAKRAVARTHY, S. R. 1987 Uniformly high order accurate essentially non-oscillatory schemes, III. *J. Comp. Phys.* **71,** 231-303.

LEE, S., LELE, S. K., & MOIN, P. 1991 Eddy shocklets in decaying compressible turbulence. *Phys. Fluids A.* **3,** 657-664.

LEE, S., MOIN, P., & LELE, S. K. 1992 Interaction of isotropic turbulence with a shock wave. *Report TF-52*, Department of Mechanical Engineering, Stanford University.

LILLY, D. K. 1992 A proposed modification of the Germano subgrid-scale closure method. *Phys. Fluids A.* **4,** 633-635.

MOIN, P., SQUIRES, K., CABOT, W., & LEE, S. 1991 A dynamic subgrid-scale model for compressible turbulence and scalar transport. *Phys. Fluids A.* **3,** 2746-2757.

ROGERSON, A. & MEIBURG, E. 1990 A numerical study of the convergence properties of ENO schemes. *J. Sci. Comp.* **5,** 151-167.

SHERMAN, F. S. 1955 A low-density wind-tunnel study of shock-wave structure and relaxation phenomena in gases. *NASA TN-3298.*

SHU, C.-W. 1990 Numerical experimentation on the accuracy of ENO and modified ENO schemes. *J. Sci. Comp.* **5,** 127-149.

SHU, C.-W., ERLEBACHER, G., ZANG, T. A., WHITAKER, D., & OSHER, S. 1992 High-order ENO schemes applied to two- and three-dimensional compressible flow. *Appl. Num. Math.* **9,** 45-71.

SHU, C.-W. & OSHER, S. 1989 Efficient implementation of Essentially Non-oscillatory shock-capturing schemes, II. *J. Comp. Phys.* **83,** 32-78.

SMAGORINSKY, J. 1963 General calculation experiments with the primitive equations. I. The basic experiment. *Mon. Weather Rev.* **91,** 99-164.